

1 **Significant recent warming over the northern Tibetan**
2 **Plateau from ice core $\delta^{18}\text{O}$ records**

3

4 **Wenling An¹, Shugui Hou^{1,5*}, Wangbin Zhang¹, Yetang Wang², Yaping Liu³, Shuangye Wu^{1,4},**
5 **Hongxi Pang¹**

6 1 Key Laboratory of Coast and Island development of Ministry of Education, School of
7 Geographic and Oceanographic Sciences, Nanjing University, Nanjing 210093, China

8 2 College of Population, Resources and Environment, Shandong Normal University, Jinan 250014,
9 China

10 3 State Key Laboratory of Cryospheric Science, Cold and Arid Regions Environmental and
11 Engineering Research Institute, Chinese Academy of Sciences, Lanzhou 730000, China

12 4 Geology Department, University of Dayton, Ohio 45469-2364, USA

13 5 CAS Center for Excellence in Tibetan Plateau Earth Sciences, Beijing 100101, China

14 * Correspondence to: S. Hou (shugui@nju.edu.cn)

15

16

17

18

19

20

21

22

23 **Abstract:** Stable oxygen isotopic records in ice cores provide valuable information about past
24 temperature, especially for regions with scarce instrumental measurements. This paper presents
25 the $\delta^{18}\text{O}$ result of an ice core drilled to bedrock from Mt. Zangser Kangri (ZK), a remote area on
26 the northern Tibetan Plateau (TP). We reconstructed the temperature series for 1951-2008 from the
27 $\delta^{18}\text{O}$ records. In addition, we combined the ZK $\delta^{18}\text{O}$ records with those from three other ice cores
28 in the northern TP (Muztagata, Puruogangri and Geladaindong) to reconstruct a regional
29 temperature history for the period 1951-2002 (RTNTP). The RTNTP showed significant warming
30 at $0.51\pm 0.07^{\circ}\text{C}(10\text{yr})^{-1}$ since 1970, a higher rate than the trend of instrumental records of the
31 northern TP ($0.43\pm 0.08^{\circ}\text{C}(10\text{yr})^{-1}$) and the global temperature trend ($0.27\pm 0.03^{\circ}\text{C}(10\text{yr})^{-1}$) at the
32 same time. In addition, the ZK temperature record, with extra length until 2008, seems to suggest
33 that the rapid elevation-dependent warming continued for this region during the last decade, when
34 the mean global temperature showed very little change. This could provide insights into the
35 behavior of the recent warming hiatus at higher elevations, where instrumental climate records are
36 lacking.

37

38

39

40

41

42

43

44

45 **1. Introduction**

46 With an average elevation over 4000 m a.s.l., the Tibetan Plateau (TP) is the highest and most
47 extensive highland in the world. In recent decades, it has experienced rapid warming and drastic
48 environmental changes such as fast glacier retreat and land deterioration (Yao et al., 2012). In
49 recent years, the global average surface temperature has experienced relatively little change in
50 recent years (Easterlin and Wehner, 2009), whereas accelerated warming continued on the TP for
51 the same period of time (Yan and Liu, 2014; Duan and Wu, 2015). However, the rapid warming
52 trend over the Plateau was established with data from meteorological stations located at relatively
53 low elevations, and warming trend for higher elevation regions remains uncertain.

54 In addition, spatial biases also exist in the TP temperature records. Most instrumental records
55 as well as various paleoclimate proxies are located in the eastern and southern Plateau (Thompson
56 et al., 2000; B. Yang et al., 2014; Herzschuh et al., 2010; Pu et al., 2011). There is generally a lack
57 of climate data in the northern, and particularly in the northwest TP, where meteorological stations
58 were sparse, and long-term high-resolution climate records were difficult to obtain because of the
59 formidable terrain and harsh environment. However, the northern TP (Fig. 1) is a climatologically
60 important region involving complicated interactions between the mid-latitude westerlies and the
61 subtropical Asia monsoon circulation. It may serve as a bridge linking the high and low latitude
62 climatic processes (Y. X. He et al., 2013). It is therefore essential to evaluate the extent and
63 magnitude of regional climate changes over this region without coverage bias.

64 The ice core $\delta^{18}\text{O}$ is an important paleoclimate proxy on the TP (Thompson et al., 2000; Qin
65 et al., 2002), and has been generally considered to be a reliable indicator for past temperatures
66 (Yao et al., 2006; Joswiak et al., 2010). However, great discrepancies still exist among different

67 temperature reconstructions and instrumental records owing to the distinct geographic locations
68 and atmospheric circulation conditions (Liu and Chen, 2000; N. Wang et al., 2003; Y. Q. Wang et
69 al., 2003; Yao et al., 2006). Therefore, it is important to establish more high resolution temperature
70 records on the TP, particularly over such extensive high elevation regions as the northern TP, in
71 order to evaluate the warming trends at high elevations in light of the recent warming hiatus. In
72 this study, we measured the $\delta^{18}\text{O}$ values in an ice core drilled from the Zangser Kangri (ZK)
73 glacier on the northern TP, from which temperature changes in the past decades could be
74 established. The ZK ice core $\delta^{18}\text{O}$ records made it possible to study the past climate variations
75 over a relatively inaccessible part of the TP, where instrumental records are very limited. In
76 addition, we also established the regional climate change history by combining ZK with the $\delta^{18}\text{O}$
77 records from other ice cores in the northern TP.

78

79 **2 Methodology and Data**

80 **2.1 Research area and ice core dating**

81 The ZK glacier is located in the northwest part of the TP, covering an area of 337.98 km²
82 with a volume of 41.70 km³ (2005 data, Shi, 2008). The snowline is about 5700~5940 m a.s.l.. In
83 the April of 2009, two ice cores to bedrock (127.7m and 126.7m in length for Core 1 and Core 2
84 respectively) were recovered from the glacier (34°18'05.8"N, 85°51'14.2"E, 6226 m a.s.l., Fig.1).
85 The glacier temperature ranged from -15.2°C to -9.2°C, with a mean temperature of -11.7°C,
86 -12.4°C at 10 m depth and a basal temperature of -9.2°C.

87 These two ice cores were kept frozen and transported to the State Key Laboratory of
88 Cryospheric Sciences, Cold and Arid Regions Environmental and Engineering Research Institute,

89 Chinese Academy of Sciences for processing. This study was based upon the analysis of Core 1. A
90 total of 2884 samples were taken from Core 1 at a resolution of 4~6 cm. The outer ~2 cm of each
91 sample was removed for stable oxygen isotope analysis. The inner portion of the ice core was
92 collected in pre-cleaned polyethylene sample containers for chemical and dust particle analyses.
93 Stable oxygen isotope ratio ($\delta^{18}\text{O}$) was determined using a Picarro Wavelength Scanned Cavity
94 Ring-Down Spectrometer (WS-CRDS, model L2120i). Major cations and anions were analyzed
95 using a Dionex-600 and ICS-2500 ion chromatograph respectively.

96 In the northern TP, the annual cycle of $\delta^{18}\text{O}$ along the ice core profile is primarily related to
97 temperature variations (Araguás-Araguás et al., 1998; Yao et al., 2013). The $\delta^{18}\text{O}$ compositions in
98 modern precipitation samples collected at northern TP show marked seasonal patterns with the
99 high values in summer and low values in winter (Yu et al., 2009). In addition, the major ions (e.g.,
100 Mg^{2+} and SO_4^{2-}) also show clear seasonal cycles with high concentrations in winter/spring and
101 low concentrations in summer (Zheng et al., 2010). They have been used in past studies as
102 complementary tools in ice core dating in the northern TP (Kang et al., 2007). Therefore, the ZK
103 ice core was dated by using the seasonality of $\delta^{18}\text{O}$ in conjunction with the seasonal variations of
104 major ions, including Mg^{2+} , Ca^{2+} and SO_4^{2-} , with a reference layer of β activity peak in 1963 (Fig.
105 2). The core 1 was dated back to 1951 at 16.38 m depth with uncertainty estimated within 1 year
106 (Fig. 2, Zhang et al., 2016). Based on the dating result and density of the ice core profile, the mean
107 annual net accumulation rate was estimated to be low for ZK glaciers ($190 \text{ kg H}_2\text{O m}^{-1} \text{ yr}^{-1}$). This
108 study focused on the $\delta^{18}\text{O}$ records in the top 16.38 m of the ice core, corresponding to the time
109 period 1951-2008.

110

111 **2.2 Climate data**

112 The ZK glacier is located at a transition zone with shifting influences between the westerlies
113 and the Indian summer monsoon (Yao et al., 2013). Based on the climate records from the two
114 nearby meteorological stations, at Gêrzê (32°09', 84°25', 4414.9m a.s.l., 1973-2008) and Xainza
115 (30°57', 88°38', 4800m a.s.l., 1961-2008) (Fig. 1), the local mean monthly temperature ranges
116 from -10.8°C in January to 10.7°C in July, with an annual average of 0°C. Precipitation averages
117 257 mm per year, of which 75% falls between June and September (Fig. S1a).

118 In order to establish the representativeness of the ZK ice core $\delta^{18}\text{O}$ for the regional climate,
119 we performed correlation analysis, using Pearson's correlation coefficient (r), between the ice core
120 $\delta^{18}\text{O}$ time series and temperature records from the nearby meteorological stations (Gêrzê and
121 Xainza), and the instrumental temperature series from a network of meteorological stations in the
122 northern TP (hereafter, ITNTP). The ITNTP time series was derived from 14 climate stations used
123 in Guo and Wang (2011), and was extended to 2014 based on the data provided by the Data and
124 Information Center, China Meteorological Administration. It should be noted that most of the
125 stations used in ITNTP time series were located on the eastern part of the northern TP with
126 altitudes ranging from 2767 to 3367 m (Guo and Wang, 2011), whereas this study focused on the
127 higher (> 5700 m) and more extensive western part of the northern TP (Fig. 1). In addition, spatial
128 correlations were carried out between ZK $\delta^{18}\text{O}$ and the CRU 4 gridded temperature reanalysis data
129 (Mitchell and Jones, 2005) on the KNMI Climate Explorer (<http://climexp.knmi.nl>).

130 In this study, in addition to the ZK series, we also attempted to reconstruct a regional
131 temperature series by combining ZK with other ice core $\delta^{18}\text{O}$ records in the northern TP, including
132 Muztagata (Tian et al., 2006), Puruogangri (Yao et al., 2006), Geladaindong (Kang et al., 2007)

133 and Malan (N. Wang et al., 2003) (Fig. 4 and Table 2). We first examined the consistency of these
134 ice core records and excluded Malan from the reconstruction because of its drastically different
135 temporal patterns from the rest of the records. To combine the remaining 4 ice core records, we
136 derived the $\delta^{18}\text{O}$ anomalies for each ice core series to eliminate the difference in the absolute
137 values, and calculated their average (Fig. S2), which was then used to reconstruct the regional
138 temperature time series.

139

140 **3 Results and Discussion**

141 **3.1 The ZK ice core $\delta^{18}\text{O}$ variation and its relationship with regional** 142 **meteorological data**

143 The raw $\delta^{18}\text{O}$ values throughout the ZK ice core profile from 1951 to 2008 were presented in
144 Figure 2. For this section, the $\delta^{18}\text{O}$ values ranged from -17.65‰ at 13.8 m to -3.79‰ at 6.85 m,
145 with an average value of -10.97‰ (Fig. 2). The $\delta^{18}\text{O}$ values were relatively low in the 1960s,
146 followed by an increasing trend from 1970s to the end of the record.

147 Stable oxygen isotope in precipitation could be affected by a variety of environmental factors.
148 In addition to temperature, the $\delta^{18}\text{O}$ values in ice cores could also be affected by precipitation
149 seasonality and amount (Dansgaard, 1964). To exclude possible influence of precipitation, we first
150 examined whether the seasonal distribution of precipitation experienced any significant changes
151 during the study period by using the precipitation records from the two nearby stations. Results
152 showed weak positive trends for the proportion of precipitation in winter and spring, and no
153 statistically significant trends for the proportions of precipitation in summer and fall (Fig. S1b and
154 c). This suggests that changes in seasonal distribution of precipitation did not exert a major

155 influence on the $\delta^{18}\text{O}$ values in ZK ice cores during the period 1961-2008. Besides, we found no
156 significant correlation between the ZK $\delta^{18}\text{O}$ record and precipitation amount recorded at the
157 stations (Table S1). Partial correlation analysis showed this to be true even when annual
158 temperature was controlled ($r_{\text{partial}} = 0.01$, $p > 0.1$). This suggests that precipitation amount had
159 little influence on the ZK $\delta^{18}\text{O}$ values.

160 On the other hand, the ZK $\delta^{18}\text{O}$ time series showed positive correlation with annual
161 temperature measured at each of the nearby stations ($r = 0.31$, $p = 0.07$ for the Gêrzê station; $r =$
162 0.43 , $p = 0.002$ for the Xainza station), the mean annual temperature of the two stations ($r = 0.34$,
163 $p = 0.01$), and ITNTP ($r = 0.35$, $p = 0.02$) (Table 1). Stronger correlation existed between the ZK
164 $\delta^{18}\text{O}$ and spring (March-May) temperature of the stations (Table 1). Linear regressions led to a
165 mean $\delta^{18}\text{O}$ -temperature slope of $0.85\text{‰ }^{\circ}\text{C}^{-1}$ with values ranging from 0.67 to $0.98\text{‰ }^{\circ}\text{C}^{-1}$ (Table
166 1). This is consistent with the published $\delta^{18}\text{O}$ -temperature relationships derived from ice cores
167 over the northern TP (X. X. Yang et al., 2014).

168 Significant spatial correlation existed between the ZK $\delta^{18}\text{O}$ series and the CRU gridded
169 temperature data in the region surrounding the drilling site. The ZK $\delta^{18}\text{O}$ series showed positive
170 correlations with annual mean and minimum temperatures for most part of the northern TP (Fig. 3).
171 The most significant and spatially extensive correlations were found between the ZK $\delta^{18}\text{O}$ and
172 spring temperatures (Fig. 3c and d), which were consistent with previous results between the ZK
173 $\delta^{18}\text{O}$ series and station temperature records (Table 1). The stronger spring temperature signal
174 recorded in ZK $\delta^{18}\text{O}$ record may be attributed to the different seasonal moisture sources in this
175 region. At Shiquanhe and Gêrzê, Yu et al. (2009) found that during the non-monsoon period
176 (October–June) when local moisture recycling and the westerlies dominate the moisture sources,

177 air temperature correlates more strongly with $\delta^{18}\text{O}$ in precipitation. On the other hand,
178 precipitation $\delta^{18}\text{O}$ in monsoon season could be affected by a variety of factors other than
179 temperature, including the convection intensity, distance from moisture sources and amount effect
180 (Y. He et al., 2015; Tang et al., 2015). This could obscure the relationship between $\delta^{18}\text{O}$ and air
181 temperatures (Joswiak et al., 2013). In addition, previous studies in the central Himalayas found
182 that high elevation areas ($> 3000\text{m.a.s.l.}$) can receive up to 40% of their annual precipitation during
183 cold season because of terrain locked low pressure systems and orographically forced precipitation
184 (Lang and Barros, 2004), a much higher percentage than that of surrounding low altitude areas of
185 the same region (Pang et al., 2014). Therefore, the ZK ice core (located at 6226 m a.s.l.) could
186 have had more cold-season (non-monsoonal) precipitation than that indicated by nearby
187 meteorological stations, located at much lower elevations. Both factors could result in a stronger
188 signal of spring temperature in the ZK ice core $\delta^{18}\text{O}$ record.

189

190 **3.2 Regional temperature reconstruction**

191 Detailed comparisons were made between the ZK $\delta^{18}\text{O}$ and the $\delta^{18}\text{O}$ time series of four
192 nearby ice cores, including Muztagata, Puruogangri, Geladaindong and Malan (Fig. 4 and Table 2).
193 The cooling around 1960s was present in all ice cores, and this was consistent with the observed
194 cold period during this time over the entire TP (Liu and Chen, 2000). Moreover, the significant
195 increasing trend from 1970s to present was observed in all except Malan ice core $\delta^{18}\text{O}$ series. We
196 calculated the Pearson correlation coefficients among these ice core $\delta^{18}\text{O}$ series (Table 3). The
197 results showed weak correlations between the annual values of these series. This lack of
198 correlation could result from the differences in location, elevation and hence local climates. It

199 could also arise from uncertainties in ice core dating. In order to reduce the impact of dating
200 uncertainties, we used the 5 year running averages instead of annual values, and these series
201 showed much stronger correlations, suggesting possible common regional climate patterns
202 preserved in these ice core series. This coherence is important when we use the average of
203 multiple sites to develop a regional composite.

204 In contrast to the rest of the ice cores, the Malan $\delta^{18}\text{O}$ record showed a cooling trend since
205 1970s (Fig. 4e). Such continuous low level of $\delta^{18}\text{O}$ could be caused by the change of local climate
206 conditions (Y. Q. Wang et al., 2003), but could also result from post-depositional processes on the
207 chemical profiles, such as summer melting, evaporation and condensation, all of which could
208 modify the relationship between ice core $\delta^{18}\text{O}$ and temperature (Hou et al., 2006). Furthermore,
209 the correlation analysis showed that the Malan time series was negatively correlated with other
210 four time series, and the negative relationships were more significant after 5 year running
211 averaging (Table 3). Therefore, we excluded the Malan record from further analysis.

212 Moreover, the correlations between Geladaindong and three other ice cores, i.e. ZK,
213 Muztagata, Puruogangri were relatively low even after 5 year running averages (Table 3). The lack
214 of correlation could be attributed to its local climate conditions (Table 3), such as the influence of
215 local convective vapor due to its more northern location (Kang et al., 2007). However, the ice
216 cores of ZK, Muztagata, Puruogangri and Geladaindong shared similar patterns of $\delta^{18}\text{O}$ variations,
217 especially their increasing trends since 1970s (Fig. 4). Moreover, regional composite with
218 Geladaindong records correlates very strongly with that without Geladaindong ($r = 0.95$,
219 1951-2002, $p < 0.0001$), and two series showed very similar temporal patterns (Fig. S2). Therefore,
220 we decided to include the Geladaindong ice core $\delta^{18}\text{O}$, so that the final regional reconstruction

221 could have larger spatial coverage to better represent the regional climate of the northern TP. The
222 regional temperature series was reconstructed for 1951-2002, the common period covered by the
223 four ice core $\delta^{18}\text{O}$ records. Meanwhile, a temperature reconstruction based solely on ZK ice core
224 $\delta^{18}\text{O}$ record was constructed for 1951-2008 to investigate the temperature variations since the late
225 1990s.

226 Before establishing the temperature reconstructions, it was necessary to derive the
227 $\delta^{18}\text{O}$ -temperature relationship to understand the magnitude of the temperature variation over the
228 northern TP. Yu et al. (2009) calculated the isotope sensitivity between monthly mean $\delta^{18}\text{O}$ values
229 in precipitation and the monthly mean temperatures at Gêrzê and Shiquanhe (Fig. 1) as 0.33 and
230 $0.37\text{‰ } ^\circ\text{C}^{-1}$ respectively. State of the art atmospheric models with integrated water isotopes
231 modeling suggested an average isotope sensitivity of $0.53\text{‰ } ^\circ\text{C}^{-1}$ for the present-day precipitation
232 falling at the grid where the ZK core was recovered (Risi et al., 2010). Tian et al. (2006) used the
233 range of 0.6 to $0.7\text{‰ } ^\circ\text{C}^{-1}$ to convert the $\delta^{18}\text{O}$ values to temperature for the Muztagata ice core.
234 The isotope sensitivity usually increases with elevation as indicated by Rayleigh-type equilibrium
235 fractionation model (Rowley et al., 2001). Kang et al. (2007) obtained $1.40\text{‰ } ^\circ\text{C}^{-1}$
236 $\delta^{18}\text{O}$ -temperature relationship from the linear regression between the 5 year running average of
237 Geladaindong $\delta^{18}\text{O}$ records and regional instrumental temperature records. In our study, the
238 strongest correlation was found between the 5 year running average of the regional $\delta^{18}\text{O}$ record
239 and ITNTP ($r = 0.89$, $p < 0.001$) (Fig. S3). The ZK $\delta^{18}\text{O}$ correlates most strongly with the 5 year
240 running average of the mean temperature from two nearby stations (Gêrzê and Xainza, $r = 0.60$, p
241 < 0.001) (Table 1). Based on these significant relationships, the isotope sensitivities were
242 determined as $1.46\text{‰ } ^\circ\text{C}^{-1}$ for the regional $\delta^{18}\text{O}$ series and $1.18\text{‰ } ^\circ\text{C}^{-1}$ for ZK $\delta^{18}\text{O}$ series, and

243 were used to reconstruct regional temperature series for the northern TP (RTNTP) and the ZK
244 temperature series respectively. Additional analysis showed that as isotope sensitivity value
245 increases, the response of decadal warming rate decreases, especially for the isotope sensitivity
246 values greater than 1.0 (Fig. S4).

247 The reconstructed regional temperature for the northern TP (RTNTP) was presented in Figure
248 5a together with the temperature reconstruction for the ZK ice core (Fig. 5b), ITNTP (Fig. 5c) and
249 the global temperature series (Fig. 5d) for comparison. We first compared the RTNTP with the
250 ITNTP, and found strong between the two temperature series ($r = 0.65$, $p < 0.001$). Spatially,
251 significant correlations also existed between the CRU gridded surface temperatures and the ITNTP
252 ($r = 0.50$ to 0.60 , $n = 42$, $p < 0.01$), as well as between CRU and the RTNTP ($r = 0.40$ to 0.60 , $n =$
253 52 , $p < 0.01$) over a large region (Fig. 6). The study area had the strongest correlations ($r > 0.50$, p
254 < 0.01). This suggested that the regional reconstruction adequately captured temperature variation
255 on the northern TP.

256

257 **3.3 Recent rapid warming trend over the northern TP**

258 The regional reconstruction was compared with the global annual temperature series (Fig. 5d)
259 and the ITNTP (Fig. 5c) in order to investigate the recent warming trend since 1970s. LOESS
260 regression was used to smooth the data and estimate the general trend. The reconstruction captured
261 the cooling period during 1960s, as well as the prominent warming since the 1970s to the end of
262 the record, with the highest rate of increase in the late 1990s (Fig. 5). For the period from 1970 to
263 2002, the RTNTP showed more rapid warming trend at the rate of $0.51 \pm 0.07^\circ\text{C}(10\text{yr})^{-1}$ than that of
264 the global temperature ($0.27 \pm 0.03^\circ\text{C}(10\text{yr})^{-1}$). The RTNTP rate was also higher than the ITNTP

265 rate of increase at $0.43\pm 0.08^{\circ}\text{C}(10\text{yr})^{-1}$ for the same time period. From 1990 to 2002, the warming
266 accelerated on the northern TP with rates of temperature increase at $0.95\pm 0.21^{\circ}\text{C}(10\text{yr})^{-1}$ for the
267 RTNTP and $0.90\pm 0.29^{\circ}\text{C}(10\text{yr})^{-1}$ for the ITNTP, much higher than the warming rate of the global
268 temperature ($0.37\pm 0.13^{\circ}\text{C}(10\text{yr})^{-1}$). These results seemed to indicate enhanced warming at the
269 high elevation regions on the northern TP.

270 Since the late 1990s, the global temperature showed very little change and even decreasing
271 trend since 2005 (Fig. 5d). The relatively flat warming trend was also recorded in the ITNTP (Fig.
272 5b). However, the ZK series revealed a continued warming trend in recent years after a brief pause
273 during the early 2000s (Fig. 5b). We calculated mean decadal annual temperature change based on
274 the LOESS regression model for all three time series (Fig. 7). For both the global temperature and
275 ITNTP series, the highest average warming rates occurred during 1990s, and then decreased
276 significantly since 1999 (Fig. 7c and d). The reduction of warming rate in the ITNTP series was
277 consistent with results by Duan and Xiao (2015), who found weaker warming trend during the
278 period 1998-2013 in the northern TP based on the instrumental temperature records. However, the
279 rates of increase remained high for the temperature records in the ZK series since 1999 (Fig. 7b),
280 in contrast to the slowdown of climate warming observed for the global mean and ITNTP
281 temperature records since 1999 (Fig. 7d). The persistent high warming rates derived from our
282 regional reconstructions seem to suggest that the elevation-dependent warming is still evident over
283 the high elevations of the northern TP despite the reduced warming rates observed at lower
284 stations in ITNTP (Fig. S5).

285 The persistent rapid warming in the northern TP could have been caused by the regional
286 radiative and energy budget changes (K. Yang et al., 2014; Yan and Liu, 2014; Duan and Xiao,

287 2015). Many studies show that the snow/ice-albedo feedback is an important mechanism for
288 enhanced warming at high elevation regions (Liu and Chen, 2000; Pepin and Lundquist, 2008;
289 Rangwala and Miller, 2012). Ghatak et al. (2014) found that the surface albedo decreases more at
290 higher elevations than lower elevations over the TP in recent years. Qu et al. (2013) observed a
291 decreasing trend for the snow/ice albedo at the Nyainquentanglha glacier region, central TP, for
292 the period 2000 to 2010. It has been found that the glacier albedo for the nine glaciers in western
293 China has decreased during the period 2000-2011, especially for the central TP (J. Wang et al.,
294 2014). For example, the glacial albedo of Dongkemadi and Puruogangri glaciers decreased at a
295 rate of 0.0043-0.0059 yr⁻¹ and 0.001-0.004 yr⁻¹ respectively. Reduced surface albedo increases the
296 surface absorption of solar radiation, and may have contributed to the continued warming over the
297 high elevation regions of the northern TP. Further research is needed to identify and quantify the
298 exact mechanisms accounting for the temperature variations over the Plateau.

299

300 **4 Conclusions**

301 This study presented a $\delta^{18}\text{O}$ time series of the ZK ice core from the northern TP, based on
302 which a temperature record was reconstructed for the period 1951-2008. Moreover, by combining
303 the ZK $\delta^{18}\text{O}$ with three other ice cores from the northern TP, a regional temperature history was
304 established from 1951 to 2002. These temperature reconstructions captured the rapid warming
305 trend since 1970, and showed continued warming since 1999 at much higher rates than those of
306 the global average temperature and the instrumental temperature records for the northern TP.

307 Possible explanations for this continued warming might lie in the regional radiative and
308 energy changes at higher elevations over the northern TP. However, the exact physical

309 mechanisms responsible for the consistently significant warming at higher elevations remain
310 unclear, partly due to the scarcity of available observations. Further studies are needed to
311 understand the specific characteristics of this warming trend on the TP, as well as the response
312 mechanisms of high elevations regions to global changes.

313

314 **Acknowledgments**

315 Thanks are due to many scientists, technicians, graduate students and porters for their hard work in
316 the field. We would also like to thank Hao Xu, Yaju Li, Chaomin Wang, Hao Hou, Rong Hua,
317 Jing He and Yanying Tang for their help in the laboratories. This work was supported by the
318 Natural Science Foundation of China (41330526, 41171052 and 41321062), and the Chinese
319 Academy of Sciences (XDB03030101-4).

320

321

322

323

324

325

326

327

328

329

330

331

332 **References**

333 Araguás-Araguás, L., Froehlich, K., and Rozanski, K.: Stable isotopic composition of precipitation
334 over southeast Asia, *J. Geophys. Res.*, 103(D22), 28721–28742, doi: 10.1029/98JD02582,
335 1998.

336 Dansgaard, W.: Stable isotopes in precipitation, *Tellus*, 16(4), 436–468,
337 doi:10.1111/j.2153-3490.1964.tb00181.x, 1964.

338 Duan, A. M., and Xiao, Z. X.: Does the climate warming hiatus exist over the Tibetan Plateau?,
339 *Scientific Reports*, 5, 13711, doi:10.1038/srep13711, 2015.

340 Easterling, D. R. and Wehner M. F.: Is the climate warming or cooling? *Geophys. Res. Lett.*, 36,
341 L08706, doi:10.1029/2009GL037810, 2009.

342 Ghatak, D., Sinsky, E., and Miller, J.: Role of snow-albedo feedback in higher elevation warming
343 over the Himalayas, Tibetan Plateau and Central Asia, *Environ. Res. Lett.*, 9, 114008,
344 doi:10.1088/1748-9326/9/11/114008 2014.

345 Guo, D. L. and Wang, H. J.: The significant climate warming in the northern Tibetan Plateau and
346 its possible causes, *Int. J. Climatol.*, 32, 1775–1781, doi: 10.1002/joc.2388, 2011.

347 He, Y. X., Zhao, C., Wang, Z., Wang, H. Y., Song, M., Liu, W. G., and Liu, Z. H.: Late Holocene
348 coupled moisture and temperature changes on the northern Tibetan Plateau. *Quaternary Sci.*
349 *Rev.*, 80, 47-57, doi:10.1016/j.quascirev.2013.08.017, 2013.

350 He, Y., Risi, C., Gao, J., Masson-Delmotte, V., Yao, T. D., Lai, C. T., Ding, Y. J., Worden, J.,
351 Frankenberg, C., Chepfer, H., and Cesana, G.: Impact of atmospheric convection on south
352 Tibet summer precipitation isotopologue composition using a combination of in

353 situmeasurements, satellite data, and atmospheric general circulation modeling, *J. Geophys.*
354 *Res.*, 120, 3852–3871, doi:10.1002/2014JD022180, 2015.

355 Herzsuh, U., Mischke, H. J., S., Zhang, C. J., and Böhner, J.: A modern pollen-climate
356 calibration set based on lake sediments from the Tibetan Plateau and its application to a Late
357 Quaternary pollen record from the Qilian Mountains, *J. Biogeogr.*, 37(4),752-766,
358 doi:10.1111/j.1365-2699.2009.02245.x, 2010.

359 Hou, S. G., Ren, J. W., and Qin, D. H.: Modification of three ice-core $\delta^{18}\text{O}$ records from an area of
360 high melt, *Ann. Glaciol.*, 43, 172-176, doi: 10.3189/172756406781812140, 2006.

361 Joswiak, D. R., Yao, T., Wu, G., Tian, L., and Xu, B.: Ice-core evidence of westerly and monsoon
362 moisture contributions in the central Tibetan Plateau, *J. Glaciol.*, 59, 56–66,
363 doi:10.3189/2013JoG12J035, 2013.

364 Joswiak, D. R., Yao, T., Wu, G., Xu, B., and Zheng, W.: A 70-yr record of oxygen-18 variability in
365 an ice core from the Tanggula Mountains, central Tibetan Plateau, *Clim. Past*, 6, 219–227, doi:
366 10.5194/cp-6-219-2010, 2010.

367 Kang, S. C., Zhang, Y. J., Qin, D. H., Ren, J. W., Zhang, Q. G., Bjorn, G., and Mayewski, P. A.:
368 Recent temperature increase recorded in an ice core in the source region of Yangtze River,
369 *Chin. Sci. Bull.*, 52(6), 825-831, doi: 10.1007/s11434-007-0140-1, 2007.

370 Lang, T. J. and Barros, A. P.: Winter storms in the central Himalayas, *J. Meteorol. Soc. Jpn.*, 82,
371 829–844, doi: 10.2151/jmsj.2004.829, 2004.

372 Liu, X. D. and Chen, B. D.: Climatic warming in the Tibetan Plateau during recent decad
373 es, *Int. J. Climatol.*, 20, 1729–1742, doi:10.1002/1097-0088(20001130)20:14<172
374 9::AID-25JOC556>3.0.CO;2-Y, 2000.

375 Mitchell, T. D. and Jones, P. D.: An improved method of constructing a database of monthly
376 climate observations and associated high-resolution grids, *Int. J. Climatol.*, 25(6), 693–712,
377 doi: 10.1002/joc.1181, 2005.

378 Pang, H., Hou, S., Kaspari, S. and Mayewski, P. A.: Influence of regional precipitation patterns on
379 stable isotopes in ice cores from the central Himalayas, *The Cryosphere*, 8, 289-301,
380 doi:10.5194/tc-8-289-2014, 2014.

381 Pepin, N., and Lundquist, J.: Temperature trends at high elevations: patterns across the globe,
382 *Geophys. Res. Lett.*, 35, L14701, doi: 10.1029/2008GL034026, 2008.

383 Pu, Y., Zhang, H. C., Wang, Y. L., Lei, G. L., Nace, T., and Zhang, S. P.: Climatic and
384 environmental implications from n-alkanes in glacially eroded lake sediments in Tibetan
385 Plateau: An example from Ximen Co, *Chin. Sci. Bull.*, 56(14), 1503–1510, doi:
386 10.1007/s11434-011-4454-7, 2011.

387 Qin, D. H., Hou, S. G., Zhang, D. Q., Ren J. W., and Kang, S. C.: Preliminary results from the
388 chemical records of an 80.4 m ice core recovered from East Rongbuk Glacier, Qomolangma
389 (Mount Everest), *Ann. Glaciol.*, 35, 278-84, doi: 10.3189/172756402781816799, 2002.

390 Qu, B.: Albedo changing and its impact factors in the glacier area of Mt. Nyainqentanglha region,
391 Beijing, University of Chinese Academy of Sciences, 35-36, 2013.

392 Rangwala, I. and Miller, J.: Climate change in mountains: a review of elevation dependent
393 warming and its possible causes, *Clim. Change*, 114, 527–47, doi:
394 10.1007/s10584-012-0419-3, 2012.

395 Risi, C., Bony, S., Vimeux, F., and Jouzel, J.: Water-stable isotopes in the LMDZ4 general
396 circulation model: Model evaluation for present - day and past climates and applications to

397 climatic interpretations of tropical isotopic records, *J. Geophys. Res.*, 115, D12118, doi:
398 10.1029/2009JD013255, 2010.

399 Rowley, D. B., Pierrehumbert, R. T., and Currie, B. S.: A new approach to stable isotope-based
400 paleoaltimetry: implications for paleoaltimetry and paleohypsometry of the High Himalaya
401 since the Late Miocene, *Earth Planet. Sci. Lett.*, 188, 253-268, doi:
402 10.1016/S0012-821X(01)00324-7, 2001.

403 Shi, Y. F.: *Concise Glacier Inventory of China*, Shanghai Science Press, 2008.

404 Thompson, L. G., Yao, T., Mosley-Thompson, E., Davis, M. E., Henderson, K. A., and Lin, P. N.:
405 A high-resolution millennial record of the South Asian monsoon from Himalayan ice cores,
406 *Science*, 289, 1916-1919, doi: 10.1126/science.289.5486.1916, 2000.

407 Tang, Y., Pang, H., Zhang, W., Li, Y., Wu, S., and Hou, S.: Effects of changes in moisture source
408 and the upstream rainout isotopes in precipitation — a case study in Nanjing, East China,
409 *Hydrol. Earth Syst. Sci.*, 19, 4293-4306, doi:10.5194/hess-19-4293-2015, 2015.

410 Tian, L. D., Yao, T. D., Li, Z., MacClune, K., Wu, G. J., Xu, B. Q., Li, Y. F., Lu, A. X., and Shen, Y.
411 P.: Recent rapid warming trend revealed from the isotopic record in Muztagata ice core,
412 eastern Pamirs, *J. Geophys. Res.*, 111, D13103, doi: 10.1029/2005JD006249, 2006.

413 Wang Y. Q., Pu, J. C., Zhang, Y. L., Sun, W. Z.: Characteristic of present warming change
414 recorded in Malan ice core, central Tibetan Plateau, *J. Glaciol. Geocryol.*, 25(2), 130-134,
415 2003 (in Chinese, with English abstracts).

416 Wang, J., Ye, B. S., Cui, Y. H., He, X. B., and Yang, G. J.: Spatial and temporal variations of
417 albedo on nine glaciers in western China from 2000 to 2011, *Hydrol. Process*, 28(9),
418 3454-3465, doi: 10.1002/hyp.9883, 2014.

419 Wang, N., Yao, T. D., Pu, J. C., Zhang, Y. L., Sun, W. Z., and Wang, Y. Q.: Variations in air
420 temperature during the last 100 years revealed by $\delta^{18}\text{O}$ in the Malan ice core from the Tibetan
421 plateau, *Chin. Sci. Bull.*, 48(19), 2134-2138, doi: 10.1360/02wd0539, 2003.

422 Yan, L. B. and Liu, X. D.: Has Climatic Warming over the Tibetan Plateau Paused or Continued in
423 Recent Years? *J. Earth Ocean Atmos. Sci.*, 1(1), 13-28, 2014.

424 Yang, B., Qin, C., Wang, J. L., He, M. H., Melvin, T. M., Osborn, T. J., and Briffa, K. R.: A
425 3,500-year tree-ring record of annual precipitation on the northeastern Tibetan Plateau, *P.*
426 *Natl. Acad. Sci. USA*, 111(8), 2903-2908, doi: 10.1073/pnas.1319238111, 2014.

427 Yang, K., Wu, H., Qin, J., Lin, C. G., Tang, W. J., and Chen, Y. Y.: Recent climate changes over the
428 Tibetan Plateau and their impacts on energy and water cycle: A review, *Global Planet.*
429 *Change*, 112, 79–91, doi: 10.1016/j.gloplacha.2013.12.001, 2014.

430 Yang, X. X., Yao, T. D., Joswiak, D., and Yao, P.: Integration of Tibetan Plateau ice-core
431 temperature records and the influence of atmospheric circulation on isotopic signals in the
432 past century, *Quaternary Res.*, 81(3), 520-530, doi:10.1016/j.yqres.2014.01.006, 2014.

433 Yao, T. D., Guo, X. J., Lonnie, T., Duan, K. Q., Wang, N. L., Pu, J. C., Xu, B. Q., Yang, X. X., and
434 Sun, W. Z.: $\delta^{18}\text{O}$ record and temperature change over the past 100 years in ice cores on the
435 Tibetan Plateau, *Science in China Series A*, 49(1), 1-9, doi: 10.1007/s11430-004-5096-2,
436 2006.

437 Yao, T. D., Masson-Delmotte, V., Gao, J., Yu, W. S., Yang, X. X., Risi, C., Sturm, C., Werner, M.,
438 Zhao, H. B., He, Y., Ren, W., Tian, L. D., Shi, C. M., and Hou, S. G.: A review of climatic
439 controls on $\delta^{18}\text{O}$ in precipitation over the Tibetan Plateau: Observations and simulations, *Rev.*
440 *Geophys.*, 51(4), 525-548, doi:10.1002/rog.20023, 2013.

441 Yao, T. D., Thompson, L., Yang, W., Yu, W. S., Gao, Y., Guo, X. J., Yang, X. X., Duan, K. Q.,
442 Zhao, H. B., Baiqing Xu, B. Q., Pu, J. C., Anxin Lu, A. X., Xiang, Y., Kattel D. B., and
443 Joswiak, D.: Different glacier status with atmospheric circulations in Tibetan Plateau and
444 surroundings, *Nature Clim. Change*, 2, 663-667, doi:10.1038/nclimate1580, 2012.

445 Yu, W. S., Ma, Y. M., Sun, W. Z., and Wang, Y.: Climatic significance of $\delta^{18}\text{O}$ records from
446 precipitation on the western Tibetan Plateau, *Chin. Sci. Bull.*, 54, 2732-2741, doi:
447 10.1007/s11434-009-0495-6, 2009.

448 Zhang, W. B., Hou, S. G., An, W. L., Zhou, L. Y., and Pang, H. X.: Variations of atmospheric dust
449 loading since 1951 AD recorded in an ice core from the North Tibet Plateau, *Annals of*
450 *Glaciology*, 57(71), doi: 10.3189/2016AoG71A559, 2016

451 Zheng, W., Yao, T. D., Joswiak, D. R., Xu, B. Q., Wang, N. L., and Zhao, H. B.: Major ions
452 composition records from a shallow ice core on Mt. Tanggula in the central Qinghai-Tibetan
453 Plateau, *Atmos. Res.*, 97(1-2), 70-79, doi:10.1016/j.atmosres.2010.03.008, 2010.

454

455

456

457

458

459

460

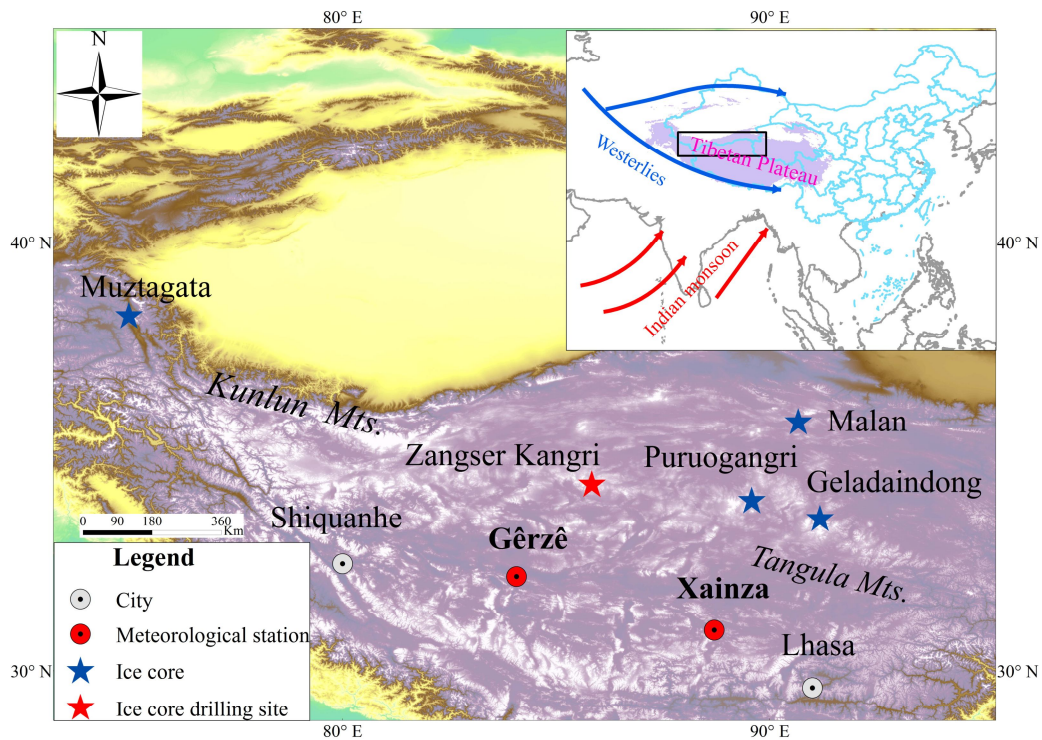
461

462

463

464 **Figures**

465 Figure 1. Location of the ice core drilling site of ZK, two nearby meteorological station sites,
466 and the location of other ice cores described in the text: Muztagata (Tian et al., 2006),
467 Puruogangri (Yao et al., 2006), Geladaindong (Kang et al., 2007) and Malan (Wang et al.,
468 2003) over the northern TP. The inset shows the relative location of the northern TP to the
469 entire TP. The black rectangle indicates the study area. Red and blue arrows represent the
470 circulation patterns for the study region. Red arrows indicate the direction of the Indian
471 monsoon (near surface) in summer, and blue arrows indicate the dominant westerlies (mid to
472 upper troposphere) in winter.



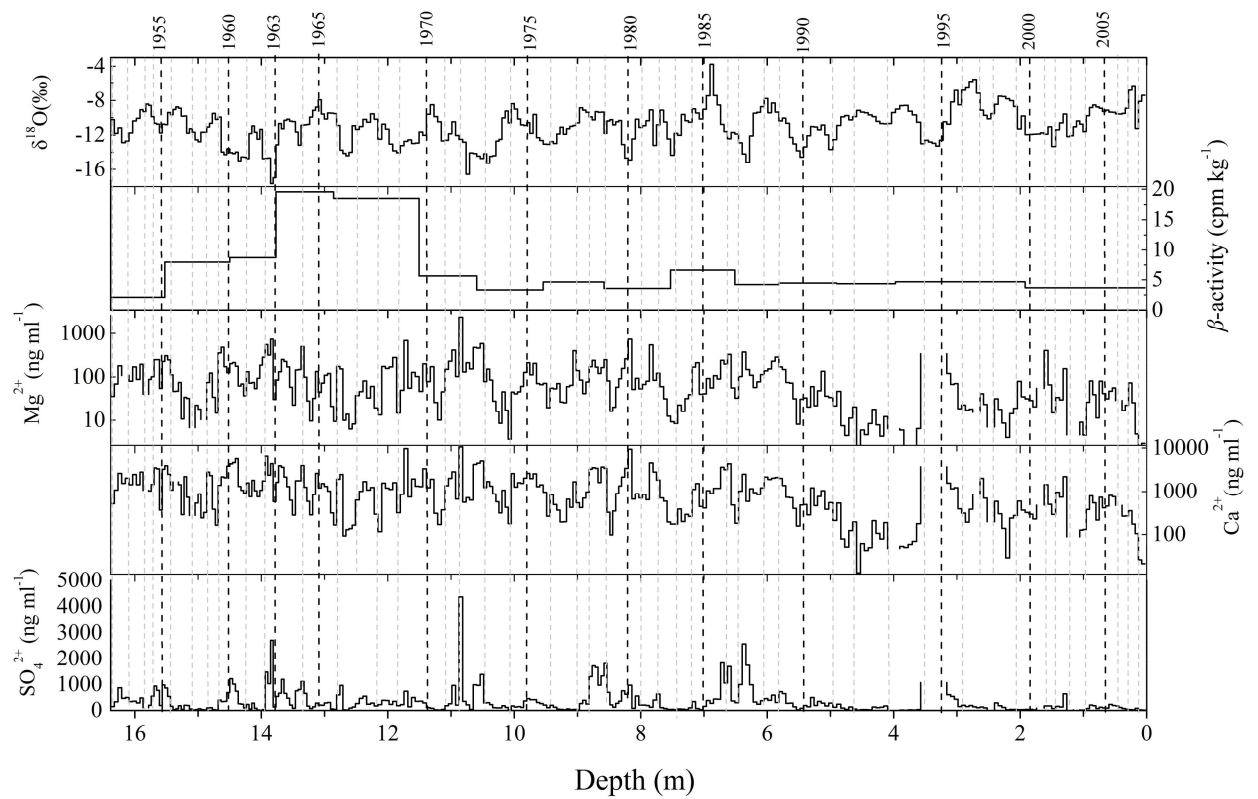
473

474 Figure 2. Variations of $\delta^{18}\text{O}$ in the ZK ice core and other data used for dating, including beta

475 activity and major ion concentrations. We calculated the logarithm to the base 10 for the

476 concentrations of the Ca^{2+} and Mg^{2+} to facilitate dating.

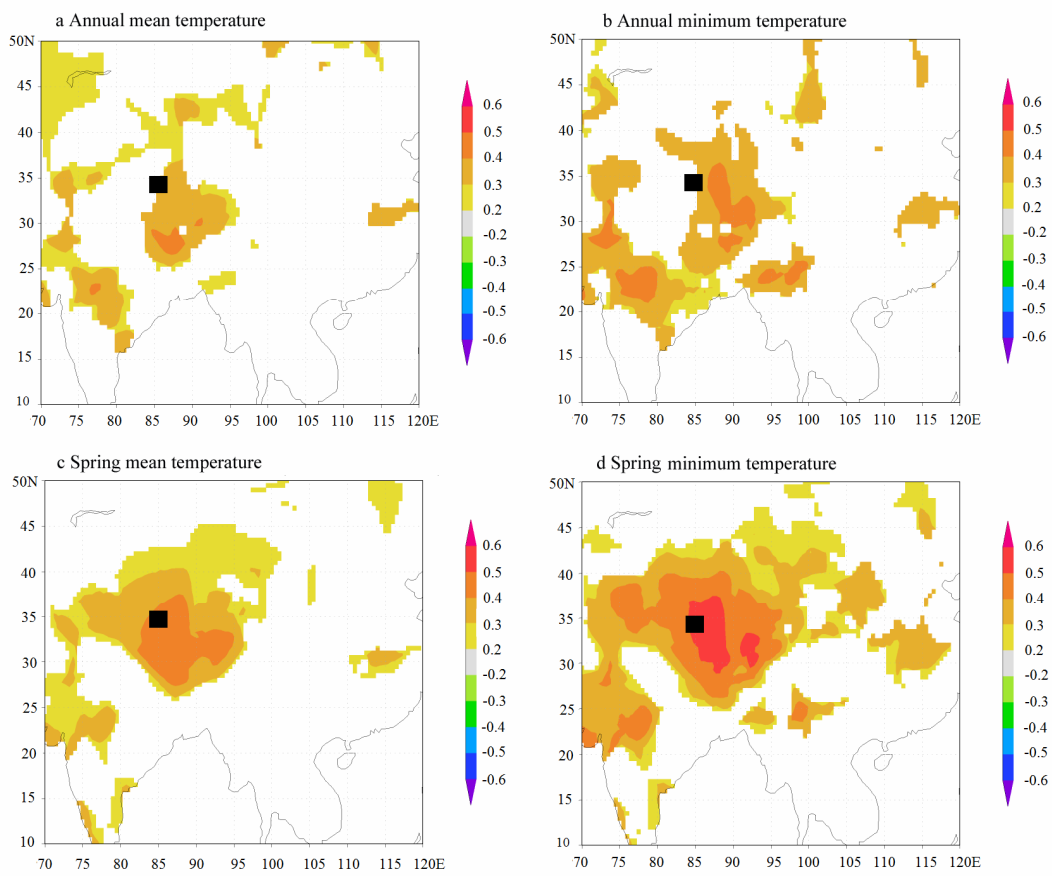
477



478

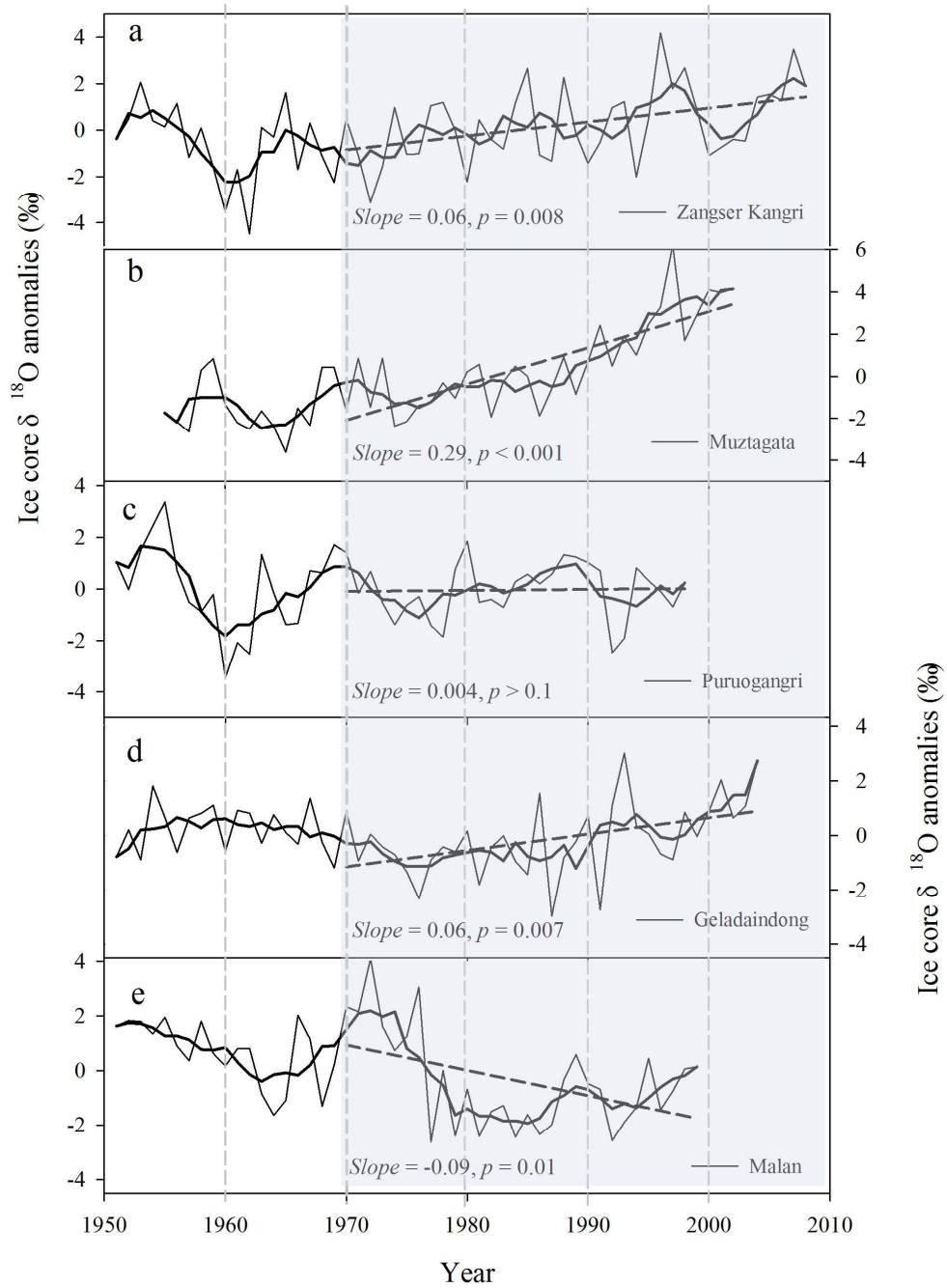
479 Figure 3. Spatial correlations of ZK ice core $\delta^{18}\text{O}$ record with CRU-gridded (Mitchell and Jones,
480 2005) annual mean temperature (a), annual minimum temperature (b), spring mean
481 temperature (c), and spring minimum temperature (d) for the period 1951-2008. Only
482 correlation coefficients significant at $p < 0.01$ are shown. The black rectangle indicates the
483 ZK ice core site.

484



485

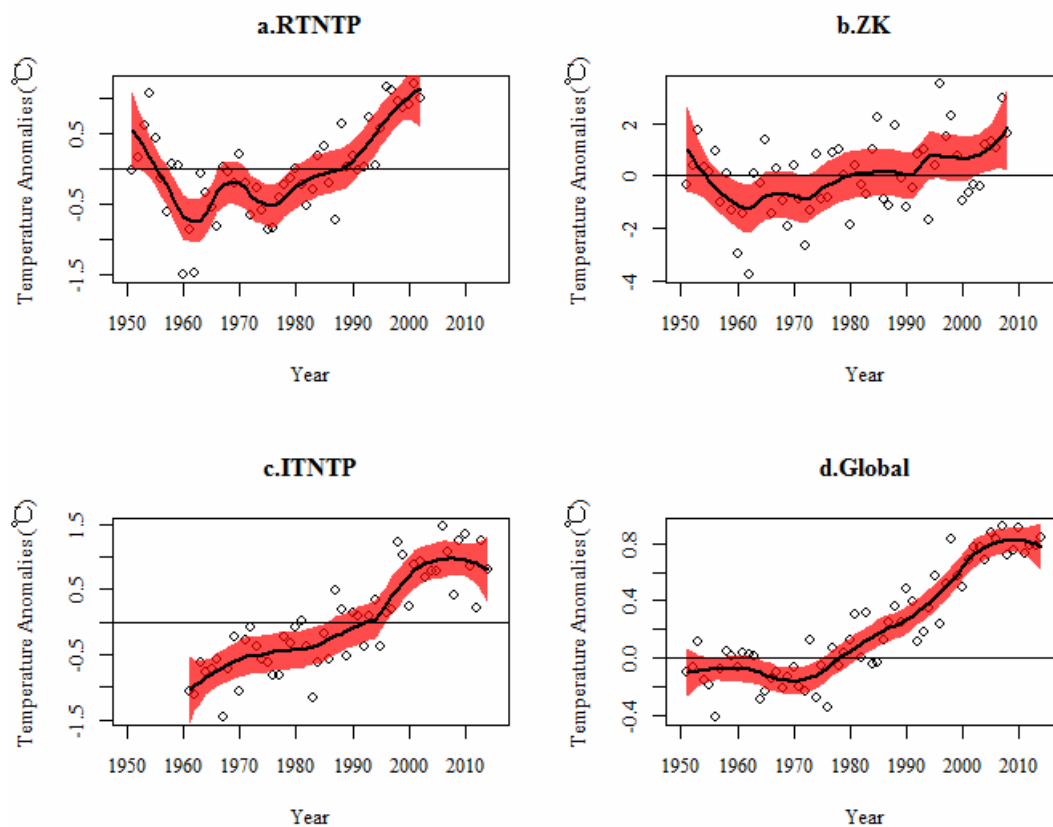
486 Figure 4. Comparison of the anomalies of $\delta^{18}\text{O}$ records in the ZK ice core (a) with $\delta^{18}\text{O}$ records
 487 from Muztagata (b), Puruogangri (c), Geladaindong (d) and Malan ice cores (e). Thin lines
 488 represent annual values, thick lines the 5-year running averages, and the dotted lines the
 489 linear trends since 1970.



490

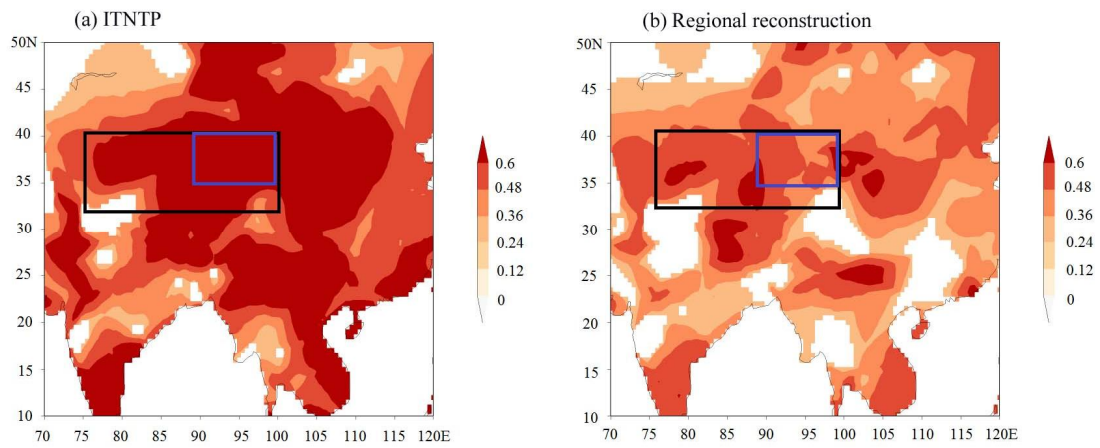
491

492 Figure 5. The reconstructed regional temperature series for northern Tibetan Plateau (RTNTP)
493 from ZK, Muztagata, Puruogangri and Geladaindong ice core $\delta^{18}\text{O}$ records (a), the
494 reconstructed temperature series from ZK ice core $\delta^{18}\text{O}$ record (b), the instrumental
495 temperature record for the northern TP (ITNTP) (c), and global average temperature (d).
496 Black trend lines were estimated using the non-parametric LOESS regression technique with
497 a span of 0.4; the dots indicate the raw values of corresponding temperature series; shading
498 represents the 95% confidence intervals of the estimated trends.



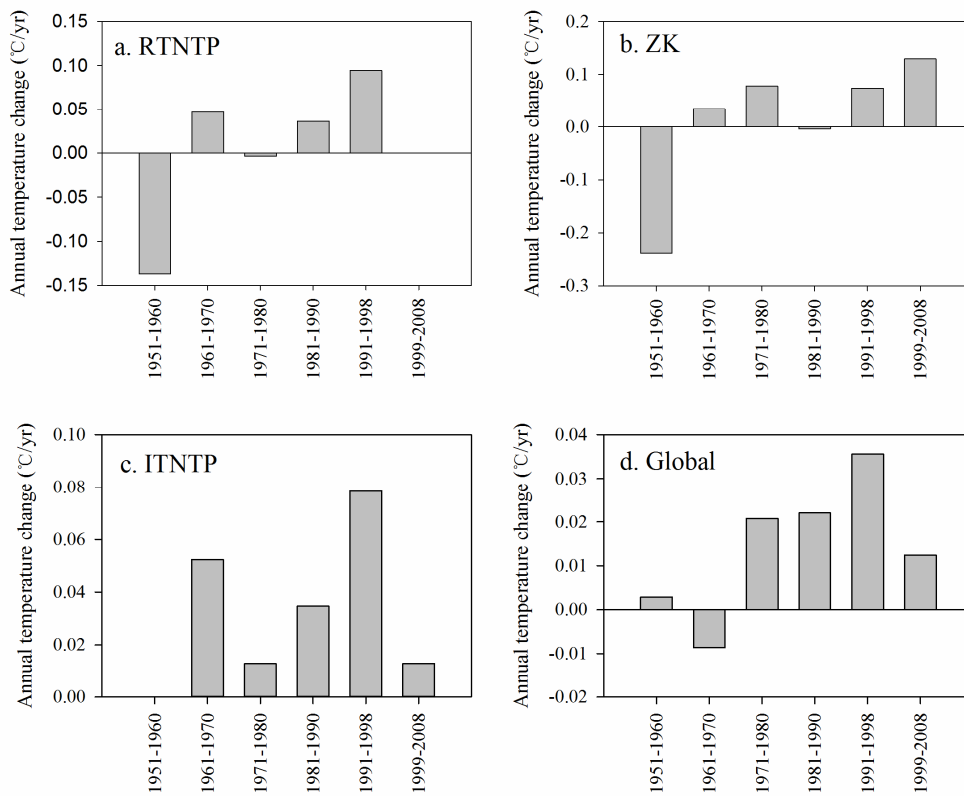
499
500
501
502
503

504 Figure 6. Spatial correlations (r values in color, $p < 0.01$) between the gridded annual mean
505 temperature data (the CRU 4 temperature time series, $0.5^\circ \times 0.5^\circ$ resolution, Mitchell and
506 Jones, 2005) and the instrumental temperature record of the northern TP (ITNTP) (Guo and
507 Wang, 2011) for the period 1961-2002 (a), and the regional temperature reconstruction series
508 for the period 1961-2002 (b). The black rectangle indicates the study area and the blue
509 rectangle indicates the region covered by ITNTP.
510



511

512 Figure 7. Decadal mean annual change rates for the regional temperature reconstruction series for
 513 northern TP (RTNTP) (a), the temperature reconstruction from ZK ice core $\delta^{18}\text{O}$ record (ZK)
 514 (b), the instrumental temperature record of the northern TP (ITNTP) (c), and global average
 515 temperature (d). The decadal mean annual change rates were estimated using the
 516 non-parametric LOESS regression model with a span of 0.4.



517
 518
 519
 520
 521
 522
 523

524 Table 1. Correlation coefficients and linear slopes between the $\delta^{18}\text{O}$ values in the ZK ice core and
 525 instrumental spring (March–May) and annual temperature from closest Gêrzê (1973–2008)
 526 and Xainza stations (1961–2008), the averaged records of the two stations (1961–2008), and
 527 the ITNTP series (1961–2008).

528

529

		Gêrzê		Xainza		Stations averaging		ITNTP
		March- May	Annual	March- May	Annual	March- May	Annual	Annual
Correlation coefficients	Annual	0.52 ^c	0.34 ^a	0.45 ^c	0.34 ^a	0.48 ^c	0.34 ^a	0.35 ^a
	5 year running average	0.63 ^c	0.53 ^c	0.73 ^c	0.60 ^c	0.73 ^c	0.60 ^c	0.61 ^c
	Slope							
	Annual	0.93 ^b	0.67 ^a	0.93 ^b	0.98 ^a	1.00 ^c	0.88 ^a	0.87 ^a
	5 year running average	0.87 ^c	0.76 ^c	1.54 ^c	1.32 ^c	1.37 ^c	1.18 ^c	0.40 ^c

530 ^a $p < 0.05$; ^b $p < 0.01$; ^c $p < 0.001$.

531

532 Table 2. Basic information of ice cores from the northern TP.

Ice core	Muztagata	ZK	Purogangri	Geladaindong	Malan
Latitude (N)	38°17'N	34°18'05.8"N	33°54'N	33°34'37.8"N	35°50'N
Longitude (E)	75°06'E	85°51'14.2"E	86°06'E	91°10'35.3"E	90°40'E
Altitude (m)	7010	6226	6200	5720	5680

533

534

535

536

537 Table 3. Correlation coefficients between the $\delta^{18}\text{O}$ values in the ZK (1951–2008), Muztagata
538 (1955–2002), Puruogangri (1951–1998), Geladaindong (1951–2004) and Malan (1951–1999) ice
539 cores, and the regional $\delta^{18}\text{O}$ values (1951–2002) averaged from ZK, Muztagata, Puruogangri and
540 Geladaindong ice cores. The values in bold are the correlation coefficients of annual values, and
541 the values in italic are the correlation coefficients of 5 year running average values
542

	ZK	Muztagata	Puruogangri	Geladaindong	Malan	Regional average
ZK		0.26	0.14	-0.02	-0.27	0.57^c
Muztagata	<i>0.68^c</i>		0.09	0.04	-0.20	0.80^c
Puruogangri	<i>0.46^c</i>	<i>0.28</i>		-0.08	0.17	0.53^c
Geladaindong	<i>-0.07</i>	<i>0.24</i>	<i>-0.12</i>		0.05	0.30^a
Malan	<i>-0.40^b</i>	<i>-0.33</i>	<i>0.14</i>	<i>0.18</i>		
Regional average	<i>0.79^c</i>	<i>0.95^c</i>	<i>0.54^c</i>	<i>0.31^a</i>		

543 ^a $p < 0.05$; ^b $p < 0.01$; ^c $p < 0.001$.

544